MULLARD LIMITED
Mullard House
Torrington Place
London, W.C.1

CONTENTS

Gunn Effect Devices and their Applications 286-293
Spark-gaps for Protection of Radio Receivers 294-295
Line Timebase and E. H. T. Trebler for Colour Tubes 296-301
Transistorised Water Level Sensor 302-304

VOL. 10 No. 100 JULY 1969

Mullard Technical Communications

VOLUME 10 NUMBER 100

July 1969

Mullard Technical Communications

VOLUME 10 NUMBER 100 July 1969

Contents

Gunn Effect Devices and their Applications *K. Wilson* 286

Spark-gaps for Protection of Radio Receivers *A. Ciuciura* 294

Line Timebase and E. H. T. Trebler for Colour Tubes *D. Gent and J. Lammers* 296

Transistorised Water Level Sensor *W. Ebbinge and D. C. de Ruiter* 302

Mullard Technical Communications records new developments in the application of electronics in science, industry, and the home. It contains information on the properties and performance of discrete and integrated semiconductor devices, electronic valves and tubes, and associated magnetic, electrical, electron-optical, and electromechanical components and assemblies. The practical circuits given are, in general, designed to provide the best working conditions and most favourable performances for the devices used. Where design principles are discussed, these may be used (so far as device ratings allow) for adaptation of the published designs to meet particular requirements. Current data sheets should always be consulted before any circuit or adaptation is considered for production.

All information is published in good faith, but no guarantee of performance is given or implied. Nor does publication imply any authority or licence for the utilisation of any patented feature.

Of the devices or assemblies included in circuits, Mullard Limited can normally supply only those listed in the Company's current catalogues. Availability in large quantities should be confirmed with Mullard Limited.

Technical enquiries should be addressed to the Editor, not to the authors or laboratories named.

Six issues are published each year. Circulation (free of charge) is limited to equipment designers, research organisations, laboratories, libraries, educational establishments, and engineering consultants. Requests for addition to the mailing list must be made on the official stationery of the establishment concerned.

Abstracts, or references to an article, should mention both the source, *Mullara Technical Communications*, and the authors. Requests for republication or translation should be made to the Editor in writing. All articles in *Mullard Technical Communications* are indexed in *British Technology Index*. Abstracts appear in *Current Papers in Physics, Electrotechnology, and Control.*

'Mullard' is the trade mark of Mullard Limited and is registered in most of the principal countries of the world.

Editor: F. A. Sowan Assistant Editor: E. G. Evans

Central Technical Services
Mullard Limited, Mullard House, Torrington Place, London, W.C.1
Telephone: 01-580 6633 Telex: 264341

© Mullard Limited, 1969

Made and Printed in England by
WIGHTMAN AND COMPANY LIMITED, 1/3 BRIXTON ROAD, LONDON, S.W.9

Gunn Effect Devices and their Applications

K. Wilson
Associated Semiconductor Manufacturers Limited, Wembley Laboratories*

The action of Gunn effect devices is described and the performance of the Mullard CXY11B Gunn device is given for various types of oscillator.

INTRODUCTION

The Gunn effect is now a well known phenomenon, having received considerable attention in laboratories in both the U.K. and the U.S.A. However, there have been considerable practical difficulties both in producing the necessary GaAs material of a high enough quality and also in fabricating satisfactory devices from this material. For these reasons there has been a noticeable lack of practical Gunn devices** on the market. Until recently the only exception was the Mullard CXY11 family; these have been available since 1966 and have been subjected to many experiments in numerous laboratories throughout the world. These devices can now be described as well understood, reliable, and practical, and are for use as microwave oscillators with the following typical performance:

frequency	8 to 12GHz (X-band, tunable)	
power output	CXY11A	5mW
	CXY11B	10mW
	CXY11C	15mW
bias requirements	7V, 1W.	

The main applications are seen as local oscillators, pump sources for parametric amplifiers, transmitters for short range doppler radars and beacons, test signal sources etc. Except where otherwise stated, this article refers to the CXY11B with 10mW output at 9·5GHz.

This article summarises the work which has been carried out on the electrical behaviour of this device in various cavity oscillators, and the principles of design for the cavities.

THE GUNN EFFECT MECHANISM

The energy band diagram of GaAs is shown in Fig.1. The conduction electrons normally lie in the main conduction band but they can be made to transfer to the satellite band if they are given sufficient energy. In the satellite band the electrons have a higher effective mass and a lower mobility. The critical energy can be attained by applying an electric field in excess of 350V/mm to the sample. This results in a characteristic for current density against electric field k as shown in Fig.2. Except for certain special designs of device, an unstable situation will exist when the sample is biased above the threshold of 350V/mm and a high field domain (E_B) will form at the cathode and drift rapidly across to the anode (Fig.3). When the domain moves out of the specimen at the anode the whole of the material will be biased at the low field E_A. The current then rises as the voltage across the specimen increases to that of the bias supply. When this voltage exceeds the threshold value once again a new domain will form at the cathode and the cycle will be repeated.

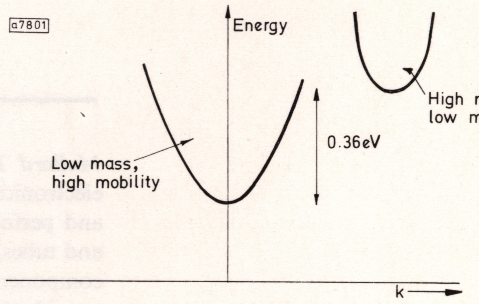

Fig. 1—Energy band diagram for n-type GaAs

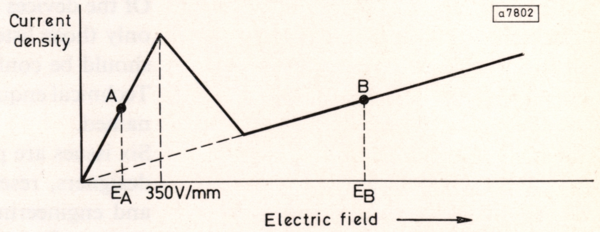

Fig. 2—Current density versus electric field characteristic of n-type GaAs

The current waveform will thus consist of the d.c. quiescent current with a series of pulses superimposed on it (Fig.4). The p.r.f. of these pulses will depend on the time taken for the domain to traverse the specimen. Since the domain velocity is about 10^8mm/s this requires a length of about 10μm for a sample intended for X-band operation.

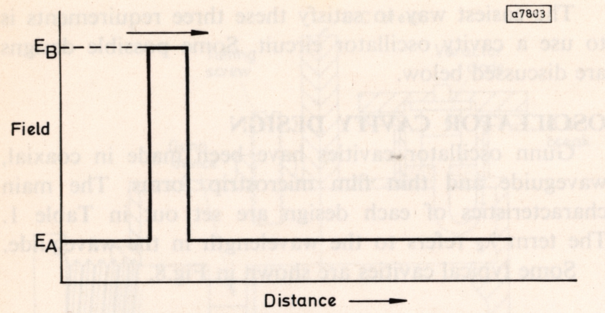

Fig. 3—Field distribution in the specimen in the presence of a domain

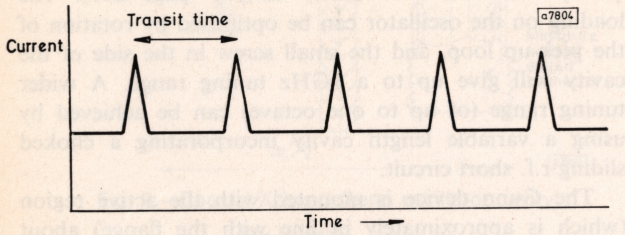

Fig. 4—Current waveform

Although the Gunn device is basically a transit time oscillator it is possible to tune the frequency by means of the external circuit over a range of one octave. This occurs because the r.f. voltage in the cavity can swing the instantaneous voltage across the device to a value below threshold and so delay the triggering of a domain until the subsequent positive half cycle of the r.f.

CONSTRUCTION OF GUNN DEVICES

The CXY11 family of Gunn effect devices are fabricated from epitaxial GaAs. This consists of a layer of n-type material grown on a low resistivity substrate. Planar techniques are used to define the area of the evaporated metal cathode contact: the substrate is used as the anode terminal. The device is mounted in a standard ceramic and metal microwave diode encapsulation, and contact to the cathode is made with thermocompression bonded gold wires. The encapsulation is completed with a projection welded end piece, thus giving a hermetically sealed device with no internal pressure contacts.

The above form of construction and the choice of contact materials to give a mechanically, metallurgically and electrically stable device have resulted in a Gunn device of very high reliability. The construction is illustrated in Fig.5.

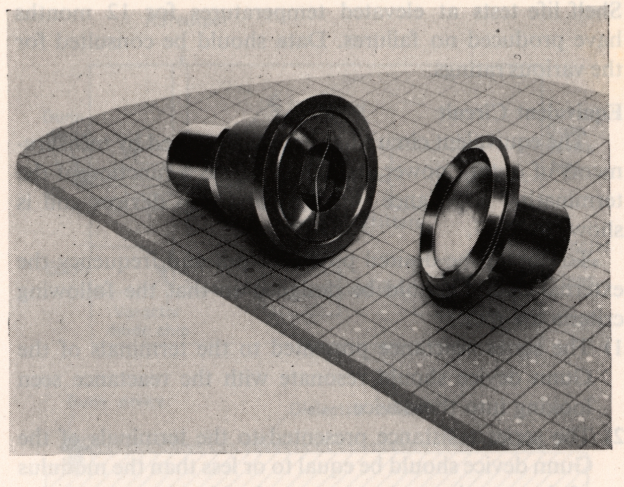

Fig. 5—Gunn device

ELECTRICAL CHARACTERISTICS

Those characteristics which are applicable to the device in isolation and are not affected by the detailed design of the oscillator cavity are described below.

D.C. Bias Characteristics

The d.c. bias characteristics are illustrated in Fig.6. At low bias levels the device appears ohmic, but when the threshold field is reached the current saturates. At higher voltages there is some fall-off in current. When the device is mounted in a cavity, slight discontinuities may be seen in the current-voltage characteristic; these are associated with the onset of r.f. oscillations. Typically the threshold bias will occur at about 4V and the saturated current will be about 130mA. It is imperative that the device should never be operated with the flange end positive.

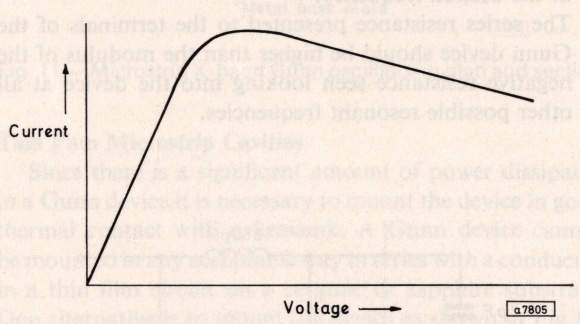

Fig. 6—D.C. characteristic of a Gunn device

There is at present a limit of 1W on the power input to the device.

The Gunn device, when biased above threshold, appears as a negative resistance in X-band and a negative resistance can also occur at certain frequencies outside X-band. It is quite common for low frequency oscillations in the range 1 to 100MHz to occur in the bias loop but these can invariably be suppressed by connecting a small capacitor of 10nF across the bias terminals at the cavity.

Electrical Ratings

$V_{b(max)} = 7V$ (flange negative only)
$P_{tot(max)} = 1W$

Life

Many of the early Gunn devices exhibited only a short life; this was the result of a lack of understanding among device designers concerning the failure mechanisms operating in the various GaAs-metal interfaces. These mechanisms have now been studied and have been eliminated from the CXY11 family, giving great reliability.

Devices in the CXY11 family have been operated continuously on life-test for 10 000 hours at the rated bias of 7V with no sign of degradation in performance. Other devices on a switched life test have withstood in excess of 10^7 on-off switching operations satisfactorily.

---

*Now G.E.C. Hirst Research Centre.

**The term Gunn device is preferred to the term Gunn diode because the device cannot be used for rectification.

Shelf life tests at elevated temperatures for 12 months have produced no failures. Data should be consulted for the various ratings.

Equivalent Circuit

The equivalent circuit has been determined by measurements of output power and frequency as a function of the terminating impedance with typical Gunn devices and is shown in Fig.7.

To obtain the desired power output and frequency the external circuit should be designed so that the following criteria are met.

1) The series reactance presented to the terminals of the Gunn device should resonate with the reactance seen looking into the device.
2) The series resistance presented to the terminals of the Gunn device should be equal to or less than the modulus of the negative resistance seen looking into the device at the desired frequency.
3) The series resistance presented to the terminals of the Gunn device should be higher than the modulus of the negative resistance seen looking into the device at all other possible resonant frequencies.

The easiest way to satisfy these three requirements is to use a cavity oscillator circuit. Some possible designs are discussed below.

OSCILLATOR CAVITY DESIGN

Gunn oscillator cavities have been made in coaxial, waveguide and thin film microstrip forms. The main characteristics of each design are set out in Table 1. The term λ_g refers to the wavelength in the waveguide.

Some typical cavities are shown in Fig.8.

Coaxial Oscillator Cavity

An outline drawing for a coaxial cavity is shown in Fig.9. The cavity length is nominally λ/2 (see also *Frequency Variation with Cavity Length* page 291). The loading on the oscillator can be optimised by rotation of the pick-up loop, and the small screw in the side of the cavity will give up to a 1GHz tuning range. A wider tuning range (of up to one octave) can be achieved by using a variable length cavity incorporating a choked sliding r.f. short circuit.

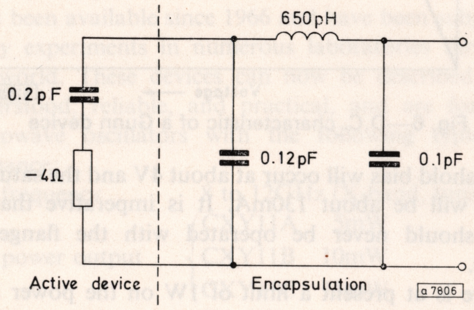

Fig. 7—Equivalent circuit of Gunn device

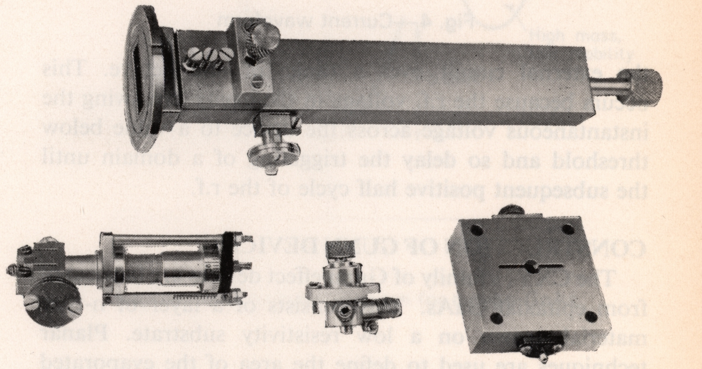

Fig. 8—Various oscillator cavities

TABLE 1

Performance of Various Cavity Oscillators

Cavity	Loaded Q	Frequency Stability with Temperature	Adjustment for Optimum Performance	A.M. Noise	F.M. Noise	Electronic Tuning Range with Varactor Diodes	Useable Mechanical Tuning Range
$\frac{\lambda}{2}$ coaxial	50 to 150	~1MHz/degC	easy	very good	adequate for most applications	up to ~700MHz	almost one octave
$\frac{\lambda_g}{2}$ waveguide	~1000	~180kHz/degC determined by cavity expansion	easy	very good	very good	~20MHz	~30%
$\frac{\lambda}{2}$ microstrip	50 to 150	~1MHz/degC	difficult	very good	adequate for most applications	up to ~700MHz in principle	no satisfactory method exists

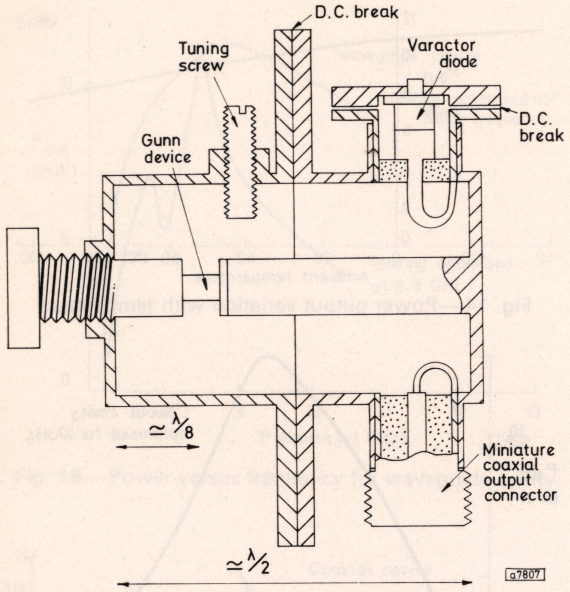

Fig. 9—Coaxial X-band Gunn oscillator cavity

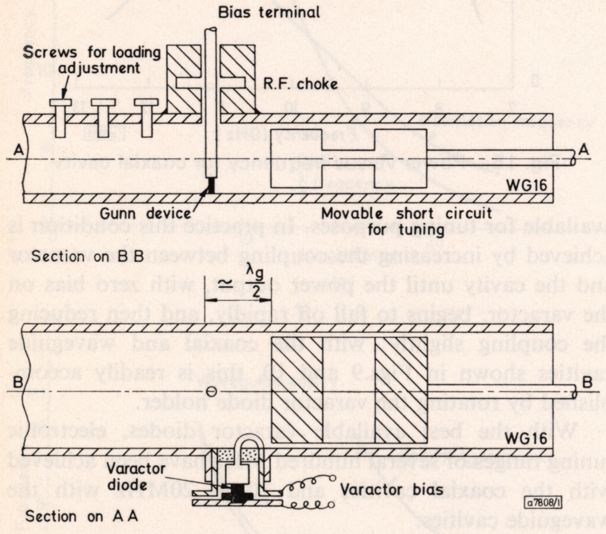

Fig. 10—Waveguide X-band Gunn oscillator cavity

The Gunn device is mounted with the active region (which is approximately in line with the flange) about λ/8 from the end of the cavity. This effectively suppresses any tendency for the cavity to oscillate in the λ mode by presenting a high resistance to the diode at the second harmonic of the desired frequency.

Waveguide Cavity

An outline drawing for a λ/2 waveguide cavity is shown in Fig.10 (see also *Frequency Variation with Cavity Length* page 291). These cavities give even better stability and noise performances than the coaxial versions but the mechanical tuning range is more restricted because of the possibility of spurious oscillations and mode jumping. Since the loaded Q of a waveguide oscillator cavity is much higher than for a coaxial cavity it is more difficult to achieve electronic tuning by means of varactor diodes or otherwise.

Where a greater electronic tuning range is required with a waveguide cavity this can be provided by decreasing the loaded Q by using reduced height waveguide for the cavity section.

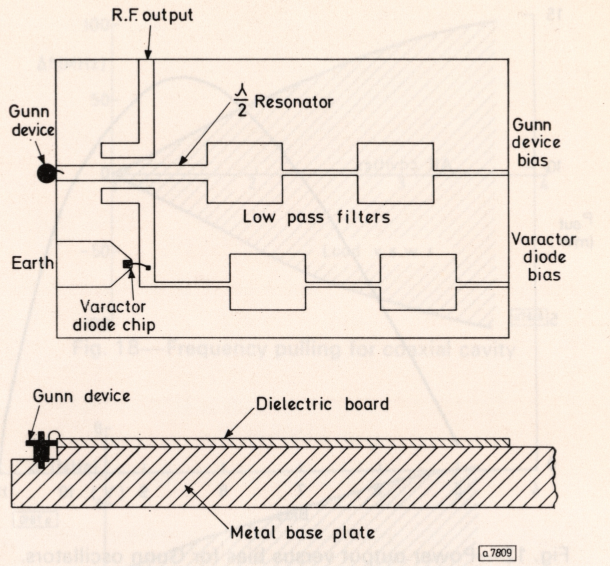

Fig. 11—Microstrip X-band Gunn oscillator in plan and section

Thin Film Microstrip Cavities

Since there is a significant amount of power dissipated in a Gunn device it is necessary to mount the device in good thermal contact with a heatsink. A Gunn device cannot be mounted in any acceptable way in series with a conductor in a thin film circuit on a ceramic or sapphire substrate. One alternative is to mount the device as shown in Fig.11, which also shows the essentials of the circuit design. Such circuits have been used to drive balanced mixers, which were constructed with the same technique, with complete success.

ELECTRONIC TUNING

There are four techniques which can be used to provide electronic tuning for a Gunn device oscillator;

1) bias supply control
2) variable permeability (ferrite) tuning
3) YIG spheres
4) varactor tuning.

Method (1) is generally unsatisfactory since the degree of frequency variation and its sign will vary from one device to another. There will also be a considerable variation in output power with frequency.

Method (2) can be used by partially filling the cavity with a suitable ferrite and varying its permeability with an external magnetic field. This can give several hundred MHz tuning range but it requires a large electromagnet and the response is slow.

Method (3) is probably capable of producing a considerable tuning range but very little work has been reported in this area.

Method (4), varactor tuning, is now well understood. It is shown in Appendix 1 that the varactor specification required is given by the equations

$$Q_{V(0)} = \frac{2.\left(\frac{C_{j(0)}}{\Delta C_j}\right)\left(\frac{\Delta f}{f}\right) Q_{Lmin}}{\frac{P_V}{P_T}}$$

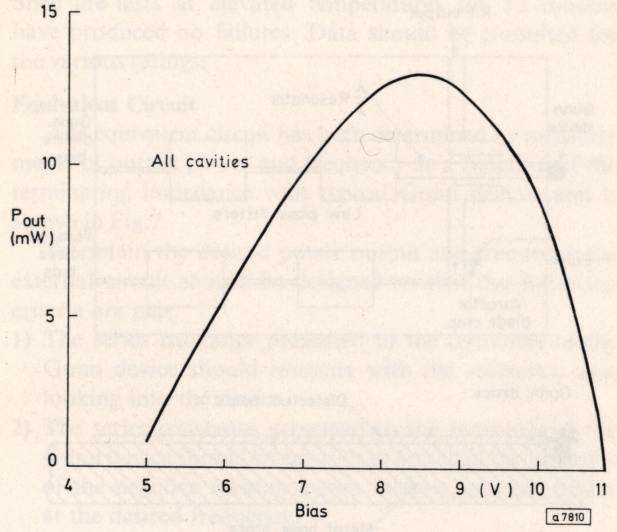

Fig. 12—Power output versus bias for Gunn oscillators. Recommended $V_{b(max)}$ is 7V

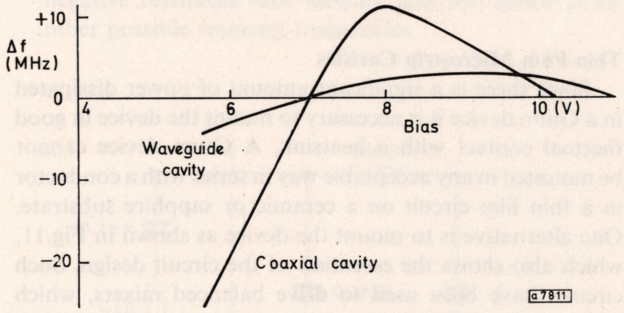

Fig. 13—Frequency versus bias for Gunn oscillators. Recommended $V_{b(max)}$ is 7V

and

$$C_{j(0)} = \frac{\left(\frac{C_{j(0)}}{\Delta C_j}\right)\left(\frac{\Delta f}{f}\right) Q_{Lmin} P_T}{V^2 \pi f}$$

where

$Q_{V(0)}$ = varactor Q at zero bias

$C_{j(0)}$ = varactor junction capacitance at zero bias

ΔC_j = varactor junction capacitance change available

Δf = electronic tuning range

f = frequency at zero bias

Q_{Lmin} = oscillator minimum loaded Q

P_V = r.f. power dissipated in the varactor

P_T = total r.f. power dissipated

V = r.m.s. voltage swing at the varactor junction.

Q_{Lmin} is determined by the rate of change of reactance presented to the device by the cavity and by the negative resistance produced by the device which in turn determines the value of load resistance which should be presented to the device.

For a λ/2 coaxial cavity $Q_{Lmin} \simeq 50$ to 150
For a λ/2 waveguide cavity $Q_{Lmin} \simeq 1000$
For a λ/2 microstrip cavity $Q_{Lmin} \simeq 50$ to 150.

It is convenient to choose a value of 0·7V for the r.m.s. voltage swing (V) at the varactor junction when using a GaAs diode or 0·4V with a silicon diode. This will mean that the varactor will be just about to conduct on the positive peaks of the r.f. when it is biased at 0V, thus enabling the whole of the reverse bias range to be available for tuning purposes. In practice this condition is achieved by increasing the coupling between the varactor and the cavity until the power output, with zero bias on the varactor, begins to fall off rapidly, and then reducing the coupling slightly; with the coaxial and waveguide cavities shown in Figs.9 and 10, this is readily accomplished by rotating the varactor diode holder.

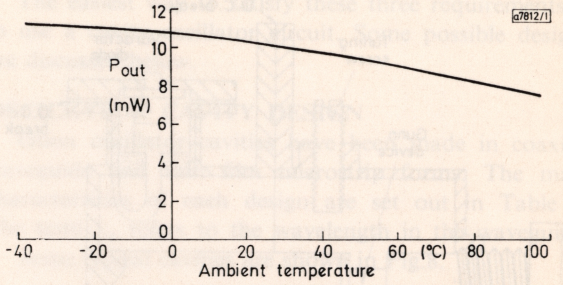

Fig. 14—Power output variation with temperature

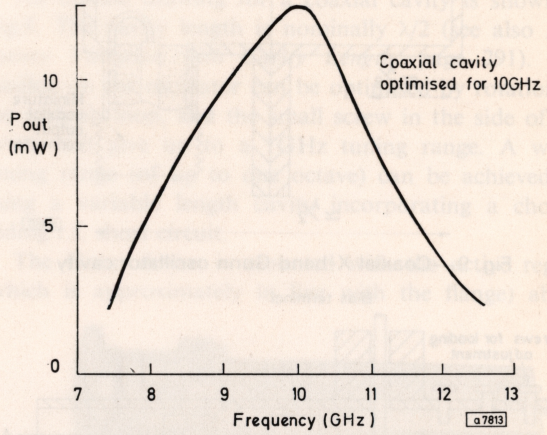

Fig. 15—Power versus frequency for coaxial cavity

With the best available varactor diodes, electronic tuning ranges of several hundred MHz have been achieved with the coaxial cavities and 10 to 20MHz with the waveguide cavities.

OSCILLATOR CHARACTERISTICS

The characteristics of various cavity oscillators containing Gunn devices are subject to some variation because of the spread in diode characteristics. The results given here are therefore only typical.

The measurements apply to typical devices giving an output power of about 10mW and working in X-band. In some cases results are quoted for operation under conditions which exceed the ratings of the CXY11B. These results are for information only and do not imply any licence to use the devices under such conditions.

Bias Supply Variations

Typical variations of output power and frequency for coaxial and waveguide cavities are shown in Figs.12 and 13. The bias, at which the frequency peaks, can occur either above or below the recommended operating voltage of 7V: for this reason, bias control is not a very satisfactory method to use for electronic tuning. The maximum sensitivity of frequency with voltage is 30MHz/V for the coaxial cavity which implies that a ripple of 1mV on the power supply will result in deviation of less than 30Hkz.

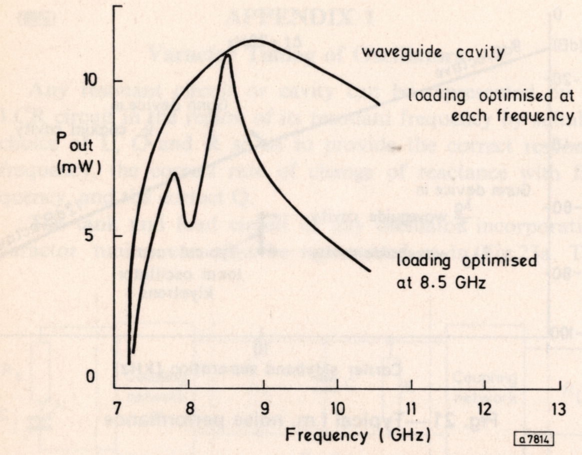

Fig. 16—Power versus frequency for waveguide cavity

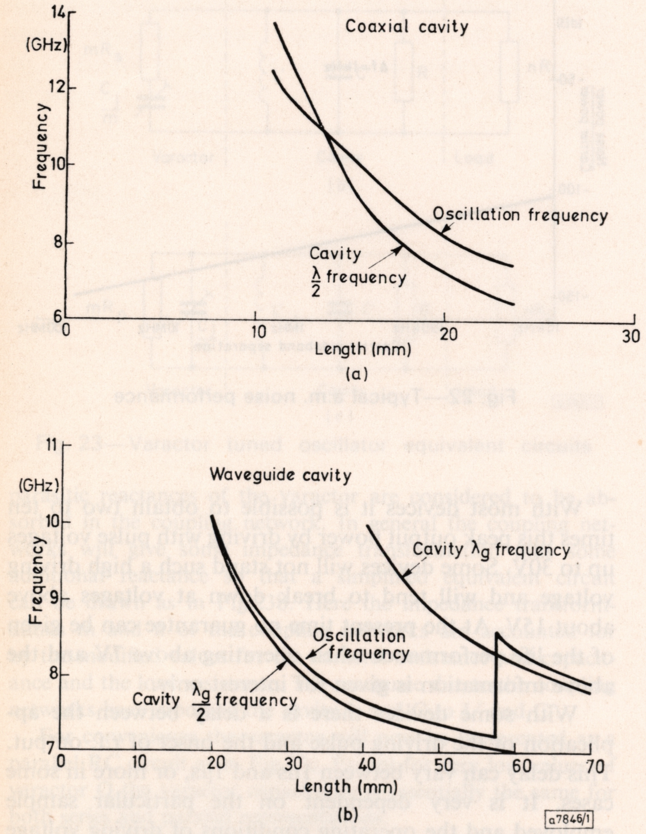

Fig. 17—Frequency versus cavity length

With the waveguide cavity this sensitivity is reduced to less than 4MHz/V.

Temperature Stability

As with all oscillators using low-Q cavities there is some variation of frequency with temperature when using a Gunn device in a λ/2 coaxial cavity. However, this dependence is only −1·5MHz/degC at worst and has a typical value of −0·75MHz/degC. The cavity expansion contributes about −0·18MHz/degC.

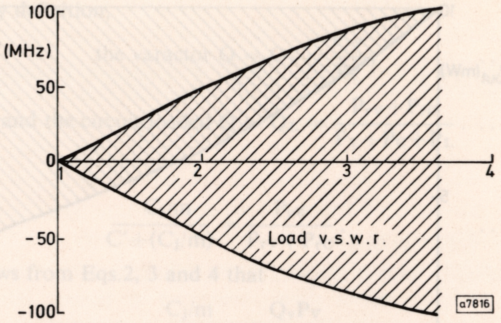

Fig. 18—Frequency pulling for coaxial cavity

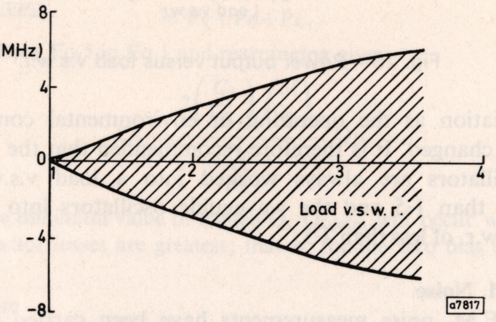

Fig. 19—Frequency pulling for waveguide cavity

For a high-Q oscillator such as the waveguide cavity, frequency variation with temperature changes is caused mainly by cavity expansion.

A typical curve of power output against temperature is given in Fig.14 which shows a variation of ±1dB from −40°C to +100°C ambient temperature. Some devices, however, show a rapid fall-off in power at low temperatures.

Power Variation with Frequency

A curve showing the variation of power output over X-band for a typical device in a wide band tunable λ/2 coaxial cavity is given in Fig.15. The loading was optimised for the centre frequency of 10GHz. It can be seen that the power variation is within ±3dB. An even flatter response can be achieved by optimising the loading at each frequency. Fig.16 shows as imilar result for the waveguard cavity.

Frequency Variation with Cavity Length

The variation of frequency with cavity length is shown in Fig.17 for coaxial and waveguide cavities. It can be seen that the cavities are exactly λ/2 long at 10·5GHz which is the frequency at which the Gunn devices are series resonant.

Effect of Load Mismatch

Figs.18, 19 and 20 show the frequency pulling and power output variation for the coaxial and waveguide cavities for load v.s.w.r. up to 3·5. The shaded areas represent the possible operating regions depending on the phase of the mismatch. If the oscillator is set up for maximum power when working into a matched load, then any increase in loading will cause the oscillator to turn off since it is a negative resistance device. For large values of v.s.w.r. it is possible to get discontinuities in the frequency

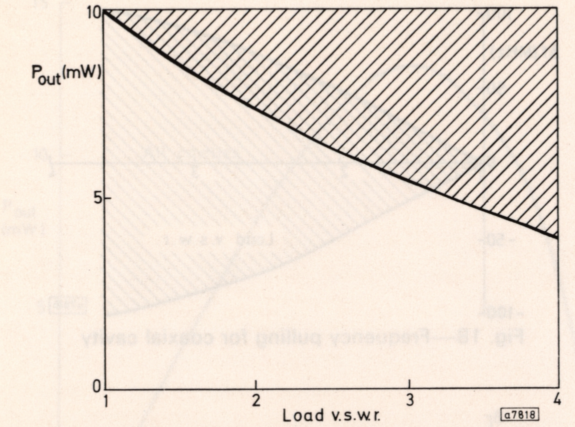

Fig. 20—Power output versus load v.s.w.r.

variation as the operating or environmental conditions are changed. It is therefore recommended that the coaxial oscillators are always worked into a load v.s.w.r. of less than 1·5 and the waveguide oscillators into a load v.s.w.r. of less than 2·5.

F.M. Noise

F.M. noise measurements have been carried out on typical devices in both coaxial and waveguide cavities and the results are shown in Fig.21.

In practice, the performance in the coaxial cavity is adequate for all applications other than doppler radar. In the waveguide cavity the performance is adequate for every application.

A.M. Noise

The a.m. noise of Gunn oscillators is very low; measurements on typical devices have shown that even in the low-Q coaxial cavity they are superior to conventional klystrons when used as local oscillators to drive single ended mixers. With a balanced mixer there is of course no detectable difference in the receiver noise figure for either type of local oscillator. A typical noise performance is shown in Fig.22.

Frequency Locking

It is possible to injection-lock a Gunn oscillator with a reference signal. The locking range Δf/f which is obtainable is given by Adler's theory as

$$\frac{\Delta f}{f} = \frac{1}{2Q_L}\sqrt{\left(\frac{P_i}{P_o}\right)}$$

where

Q_L = oscillator loaded Q
P_o = output power
P_i = power of the injected signal.

This suggests a locking range of about 10MHz at X-band for the coaxial cavity with an injection ratio of about −20dB, and this has been achieved in practice.

Pulsed Operation

It is possible to operate the CXY11 family of devices under pulsed conditions. If the pulse voltage is limited to 7V the peak output power will be no more than the c.w. output power at 7V bias.

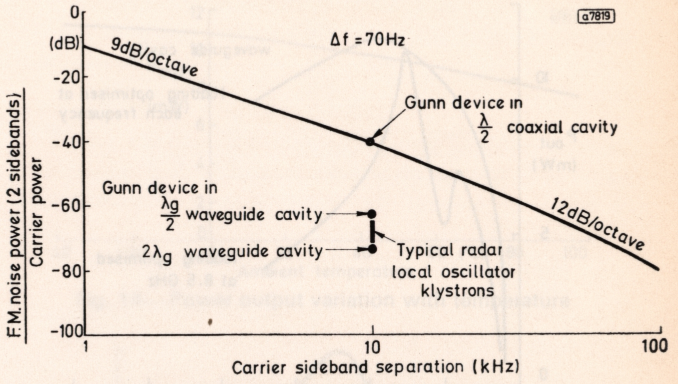

Fig. 21—Typical f.m. noise performance

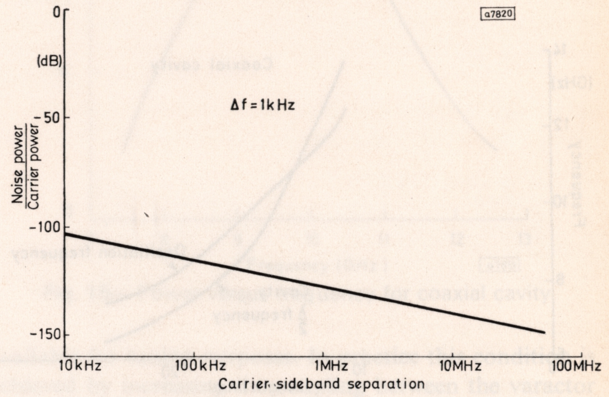

Fig. 22—Typical a.m. noise performance

With most devices it is possible to obtain two to ten times this peak output power by driving with pulse voltages up to 30V. Some devices will not stand such a high driving voltage and will tend to break down at voltages above about 15V. At the present time no guarantee can be given of the life performance when operating above 7V and the above information is given for interest only.

With some devices there is a delay between the application of the driving pulse and the onset of r.f. output. This delay can vary between 1ns and 1μs, or more in some cases. It is very dependent on the particular sample employed and the operating conditions of driving voltage and r.f. loading.

Once oscillation has commenced the rise time of the r.f. output is determined mainly by the loaded Q of the oscillator. This rise time is only a few ns for a low-Q cavity such as the λ/2 coaxial oscillator.

ACKNOWLEDGEMENTS

The author would like to thank his colleagues for all the work that made this article possible and in particular to thank Mr. F. Warner of R.R.E. Malvern who originated many of the ideas on which the work was based. This work was done in part under CVD contracts and is published by permission of The Ministry of Defence (Navy Department).

APPENDIX 1

Varactor Tuning of Oscillators

Any resonant circuit or cavity can be represented by an LCR circuit in the region of its resonant frequency by suitable choice of L, C and R so as to provide the correct resonant frequency, the correct rate of change of reactance with frequency, and the correct Q.

The tank and load circuit of any oscillator incorporating varactor tuning can thus be represented as in Fig.23a. The parasitic reactances of the varactor are considered to be absorbed in the coupling network. In general the coupling networks will give some impedance transformation plus some additional reactance so that a simplified equivalent circuit can be drawn as in Fig.23b. Here the impedance transformations m and n of the coupling networks are accounted for by the modified values for the varactor resistance and capacitance and the load resistance. The reactance due to the coupling networks have modified the cavity L and C to L′ and C′.

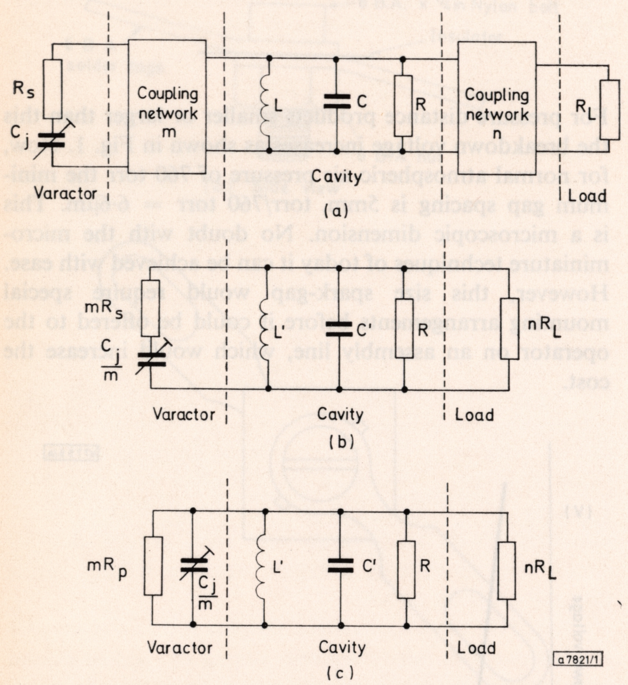

Fig. 23—Varactor tuned oscillator equivalent circuits

For convenience the varactor will now be represented as a parallel RC circuit as in Fig.23c. Except for very low values of varactor Q the varactor capacitance is essentially the same for both series and parallel representations.

Now considering Fig.23c, if:

C_j/m = transformed value of varactor capacitance
f = resonant frequency
Δf = change in resonant frequency

then for a small tuning range

$$\frac{\Delta f}{f} = \frac{1}{2}\cdot\frac{\Delta(C_j/m)}{C' + (C_j/m)}$$

$$= \frac{1}{2}\cdot\frac{\Delta C_j}{C_j}\cdot\frac{C_j/m}{C' + (C_j/m)}. \qquad \ldots(1)$$

Let

P_{rV} = reactive VA in varactor,
P_{rC} = reactive VA in cavity,
P_V = dissipated power in varactor,
P_C = dissipated power in cavity losses,
P_L = dissipated power in load.

Then by definition,

$$\text{the varactor } Q = Q_v = \frac{P_{rV}}{P_V}, \qquad \ldots(2)$$

$$\text{and the circuit loaded } Q = Q_L = \frac{P_{rV}+P_{rC}}{P_V+P_C+P_L}. \qquad \ldots(3)$$

Now

$$\frac{C_j/m}{C'+(C_j/m)} = \frac{P_{rV}}{P_{rV}+P_{rC}}. \qquad \ldots(4)$$

It follows from Eqs.2, 3 and 4 that

$$\frac{C_j/m}{C'+C_j/m} = \frac{Q_vP_V}{Q_LP_T}, \qquad \ldots(5)$$

where P_T = total dissipated power
$= P_V+P_C+P_L$.

Substituting Eq.5 in Eq.1 and rearranging gives

$$Q_v = \frac{2\left(\frac{C_j}{\Delta C_j}\right)\left(\frac{\Delta f}{f}\right)}{\frac{P_V}{P_T}}.Q_L.$$

Now the minimum value of loaded Q, Q_{Lmin}, will occur when the varactor losses are greatest; that is, for the zero bias condition.

Therefore

$$Q_{v(0)} = \frac{2\left(\frac{C_{j(0)}}{\Delta C_j}\right)\left(\frac{\Delta f}{f}\right)Q_{Lmin}}{\frac{P_V}{P_T}}. \qquad \ldots(6)$$

Note that $C_{j(0)}/\Delta C_j$ is a measure of the capacitance variation and will be a constant for a given type of varactor diode whatever the capacitance.

Eq.6 gives the zero bias Q required for the varactor in terms of the tuning range, available capacitance variation, minimum loaded Q for the oscillator, and the fraction of the r.f. power dissipated in the varactor resistance.

The required varactor capacitance can be obtained by considering the r.f. voltage swing at the varactor junction. If the r.m.s. voltage at the junction is V then at zero bias, from Eq.2

$$P_{rV} = V^2.2\pi f.C_{j(0)} = Q_{v(0)}.P_V.$$

Substituting for $Q_{v(0)}$ from Eq.6 in the above and re-arranging gives

$$C_{j(0)} = \frac{\left(\frac{C_{j(0)}}{\Delta Cj}\right)\left(\frac{\Delta f}{f}\right)Q_{Lmin}.P_T}{V^2\pi f}. \qquad \ldots(7)$$

Eq.7 gives the required varactor zero bias capacitance in terms of the available capacitance variation, the minimum loaded Q, the total r.f. power, the electronic tuning range, the r.m.s. voltage swing at the junction, and the frequency.

Generally it will be found most convenient to choose a value of $C_{j(0)}$ so that the r.f. voltage at the junction almost, but not quite, drives the varactor into forward conduction on the peaks of the cycle with the varactor bias at zero. One then has the whole of the reverse bias range of the varactor available for tuning purposes.

Eqs.6 and 7 together completely specify the varactor required for the electronic tuning of any oscillator. This theory can break down if there are additional resonances in the varactor and its coupling network occurring in the operating frequency range; however it can be shown (and is found in practice) that these are undesirable and should be avoided.

Spark-gaps for Protection of Radio Receivers

A. Ciuciura
Mullard Central Application Laboratory

Details are given of a simple spark-gap for protection of input transistors of radio receivers against damage by static charges collected on aerials.

INTRODUCTION

Static charges collected on whip aerials can damage the input transistors of radio receivers. Many devices are used to provide some degree of protection: voltage dependent resistors, back-to-back diodes, neon lamps or even a modified arrangement of the input circuit of the receiver.

This article deals with the use of spark-gaps, probably the oldest method of protection against static charges. The spark-gap provides a simple method of protection which is particularly suitable for applications in radio receivers operating on long and medium wavebands. The comparatively large inductances used on these wavelengths can ensure good breakdown conditions for the spark-gap, and the low self-capacitance of the spark-gap does not interfere with the tracking of the receiver.

With f.m. receivers the spark-gap can only be used to extend the range of protection. The basic safeguards can often be provided by increasing the impedance in the loop containing the base-emitter junction of the input transistor.

Simplicity of construction of the spark-gap described stems from the use of readily available thin sheets (or tapes) of insulating materials as spacers. Only one version is fully described in this article, but a number of variants can be derived from this basic idea to suit particular production facilities.

REQUIREMENTS

The purpose of a protective device is to direct the energy of the static discharge away from the input transistor. The device must have a low operating potential and a fast response. In addition its presence must not interfere with the operation and performance of the receiver. Under normal conditions its capacitance and conductance must therefore be low in comparison with the circuit to which it is connected.

Spark-gaps can satisfy the latter requirements easily; however, there is a limit set on the operating potential. For the application described in this article, the spark-gaps must be cheap, and this limits them to the types operating in free air. For this medium the minimum breakdown voltage is around 340V, and breakdown occurs when the product of gap spacing and air pressure is 5mm.torr[*].

For pressure distance products smaller or larger than this the breakdown voltage increases as shown in Fig. 1. Now, for normal atmospheric air pressure of 760 torr the minimum gap spacing is 5mm. torr/760 torr = 6·6μm. This is a microscopic dimension. No doubt with the micro-miniature techniques of today it can be achieved with ease. However, this size spark-gap would require special mounting arrangements before it could be offered to the operator on an assembly line, which would increase the cost.

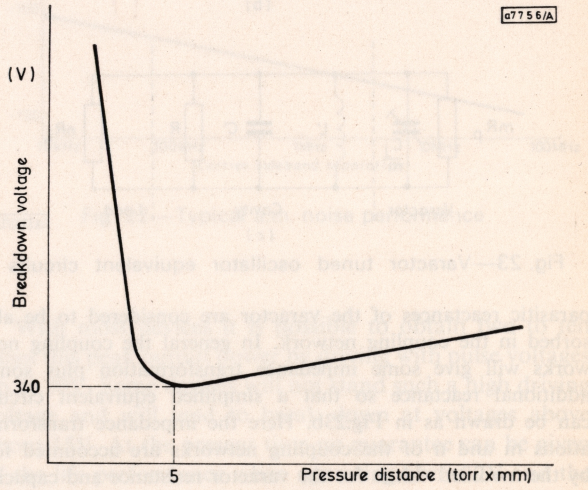

Fig. 1—Breakdown voltage as a function of p.d. product

DESCRIPTION OF SPARK-GAP

In the design of the spark-gap described below, some sacrifice in performance has been accepted in exchange for simplicity of construction. It was considered possible for an operator to handle an insulating material 25μm (0·001in) thick. Such a material, suitably perforated, forms a well defined spacer. When placed between two electrodes it provides a spark-gap with electrode separation determined by the thickness of the material.

The simplest form of spark-gap constructed on this principle is shown in Fig. 2. The electrodes consist of two 6 B.A. solder tags. Such a small size was selected to reduce self-capacitance. The spacer was formed, as shown in Fig. 2c, from 0·001in Makrofol N material. The outer dimensions are not important. The dimensions of the cut-out are dictated by two considerations: the centre hole by the diameter of the 6 B.A. bolt, and the length of the rectangular slit by the outside dimensions of the solder tags. The slit passing through the centre is made slightly larger than the eyelet so that a free access of air is provided to the electrodes. The assembly is held together by a 6 B.A. nylon bolt and a standard nut. Self-capacitance is reduced by keeping the ends of the solder tags well separated. Connecting wires could be soldered to the tags before assembly.

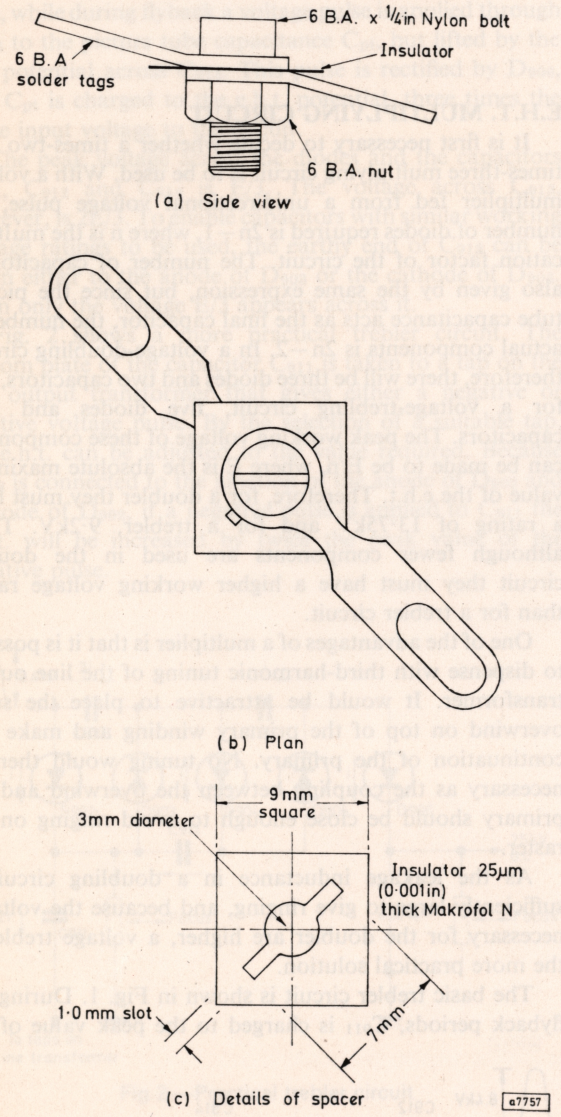

Fig. 2—Construction of spark-gap

A spark-gap of this type has a d.c. breakdown voltage of about 400V. The self-capacitance is between 8 and 10pF. The inter-electrode insulation measured after 1000 discharges from a 500pF capacitor at 15kV was in excess of 10MΩ. The performance of the spark-gap is quite unaffected by a long period of inactivity in complete darkness.

PROVISION OF BREAKDOWN CONDITIONS

For spark-gaps with simple electrode configuration, the breakdown voltage increases as the duration of applied voltage is reduced. Under pulse conditions the breakdown voltage may be many times greater than at d.c. conditions. Fortunately, this implies that the application of over-voltage increases the speed of the spark-gap. In practice, the necessary large voltage can be produced by ensuring that the discharge currents flowing into the circuit encounter some impedance. For this reason transformer coupling of the aerial circuit is preferred; with loose coupling the presence of leakage inductance will create favourable conditions for the breakdown. Conversely, where the aerial is directly connected to the tuned circuit some delay in the breakdown must be expected. However, the addition of a small coupling capacitor in series with the tuned circuit will improve the situation considerably.

MOUNTING

Any length of connecting wire between the aerial socket and the input circuit should be regarded as additional series impedance for spark-gap ignition purposes. The spark-gap should be mounted as close to the aerial socket as possible. With sockets where sufficient area of metal is available on one of the terminals, the spark-gap can be mounted directly on the terminal; the terminal can then serve as one electrode of the spark-gap.

RESULTS

The spark-gap described was tested with a number of LW/MW radio receivers. Static charges were simulated by charging a 500pF capacitor to various potentials and then connecting it directly between the aerial and earth terminals of the aerial socket. With receivers having no protection device, failure of the input transistor occurred, often after the first discharge. Receivers fitted with spark-gaps could withstand discharges up to 15kV.

Less satisfactory results were obtained with f.m. receivers because the low inductance of the input circuits provided insufficient breakdown conditions. However, with many receivers some circuit rearrangement is possible to improve these conditions. Common base configuration of the input transistor, as used in most modern receivers, can be modified by reducing the value of the emitter coupling capacitor without deterioration of performance. This also applies to the base decoupling capacitor. With the increase in the circuit impedance in the loop containing the base-emitter junction there is correspondingly less energy applied to the junction. Careful selection of components can provide safe operation for discharges up to 4 to 5kV. At this level the spark-gap becomes effective and can help to extend the range up to 10 to 15kV.

Occasionally difficulties are experienced from charges collected on various metal parts of radio receivers such as loudspeaker grilles, frames of wavechange switches, and various brackets. It is advisable, therefore, to provide a well-bonded path to d.c. between all major metal parts of the receiver and the chassis.

---

[*] 1 torr=1mm.Hg=133·322 N.m^{-2}

Line Timebase and E.H.T. Trebler for Colour Tubes

D. Gent and J. Lammers
Mullard Central Application Laboratory

A line timebase for use with Mullard 90° colour television tubes operating at an e.h.t. of 25kV is described. A voltage trebler circuit employing BY182 silicon diodes is used to generate the e.h.t. voltage.

The timebase is for 625-line operation and uses a flyback ratio of less than 18%. It is designed for mains voltage variations of ±10%.

INTRODUCTION

To stabilise the e.h.t. supply in a colour television receiver, it is usual to connect a shunt regulator valve in parallel with the picture tube. Although this arrangement can give an excellent performance, it has a number of disadvantages. Since the line timebase must supply constant e.h.t. power, unnecessary heat is generated in the line output stage when the picture tube is operating at low beam currents. As X-rays may be emitted from the e.h.t. rectifier and shunt regulator valve, the line timebase must be well screened and care must be taken to provide adequate ventilation without sacrificing the screening. These are conflicting requirements and give rise to a large screen which must cover the whole timebase. Inside this screen the timebase can dissipate 130W.

Voltages of 25kV appear at the line output transformer, e.h.t. rectifier and shunt regulator anode. Clearances between these components and the screening can must, therefore, be sufficient to prevent flashover, and so the screen must be large. The whole timebase assembly is very bulky, and is often difficult to fit conveniently into the receiver.

To operate the shunt regulator valve in a mode which gives a stable e.h.t. with mains variations and valve life deterioration, it has been necessary to generate the whole of the e.h.t. potential across the overwind (Ref.1). This results in a very large winding and has given rise to difficulties in obtaining the correct third-harmonic tuning and e.h.t. voltage because of the large overwind capacitance.

The desaturation technique has been used to help in these respects, but care must still be taken to ensure a low overwind capacitance. This necessity has led to a narrow and high winding, which is more difficult to make in production than the winding used in monochrome circuits. Because of these difficulties with the shunt regulator circuit, investigations have been made into other means of generating the e.h.t. voltage. One such method that has shown a number of advantages is a voltage multiplying circuit using semiconductor diodes.

E.H.T. MULTIPLYING CIRCUIT

It is first necessary to decide whether a times-two or a times-three multiplying circuit is to be used. With a voltage multiplier fed from a unidirectional voltage pulse, the number of diodes required is $2n-1$, where n is the multiplication factor of the circuit. The number of capacitors is also given by the same expression, but since the picture tube capacitance acts as the final capacitor, the number of actual components is $2n-2$. In a voltage-doubling circuit, therefore, there will be three diodes and two capacitors, and for a voltage-trebling circuit, five diodes and four capacitors. The peak working voltage of these components can be made to be E/n, where E is the absolute maximum value of the e.h.t. Therefore, for a doubler they must have a rating of 13·75kV and for a trebler, 9·2kV. Thus, although fewer components are used in the doubler circuit they must have a higher working voltage rating than for a trebler circuit.

One of the advantages of a multiplier is that it is possible to dispense with third-harmonic tuning of the line output transformer. It would be attractive to place the small overwind on top of the primary winding and make it a continuation of the primary. No tuning would then be necessary as the coupling between the overwind and the primary should be close enough to avoid ringing on the raster.

As the leakage inductance in a doubling circuit is sufficiently large to give ringing, and because the voltages necessary for the doubler are higher, a voltage trebler is the more practical solution.

The basic trebler circuit is shown in Fig. 1. During the flyback periods, C_{911} is charged to the peak value of the voltage appearing at the anode of D_{902}. During the scanning periods, one plate of C_{912} is taken to approximately chassis potential, while the other plate is charged to the positive voltage across C_{911}. When the flyback pulse occurs, voltage pulses are applied to D_{904} through C_{912}, but lifted by the d.c. potential across capacitor C_{913} which is therefore charged to twice the value of the input pulse at the anode of D_{902}. Similarly, C_{914} is charged through D_{905} during scanning periods to the d.c. potential across C_{913}, while during flyback a voltage pulse is applied through D_{906} to the picture tube capacitance C_{pt}, but lifted by the d.c. potential across C_{914}. This pulse is rectified by D_{906}, and C_{pt} is charged to the e.h.t. potential, three times the pulse input voltage to the circuit.

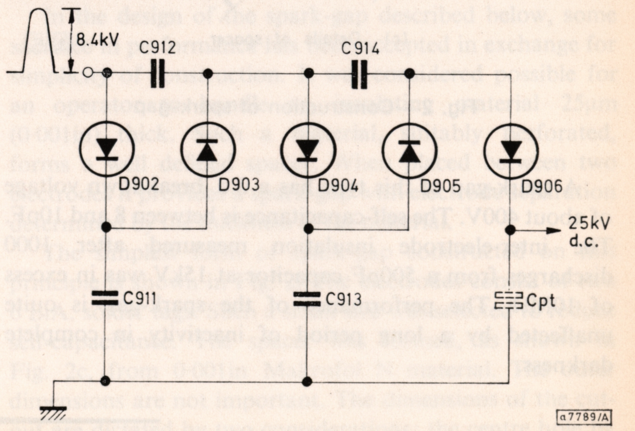

Fig. 1—Basic trebler circuit

The peak voltage across the diodes and the capacitors C_{911}, C_{912} and C_{914} is E/3. The voltage across C_{913}, however, is 2E/3. To enable capacitors with similar working voltage ratings to be used, the earthy end of C_{913} can be taken either to the anode of D_{903} or the cathode of D_{906}. Then only the voltage E/3 appears across it.

Fig. 2 shows a more practical trebler circuit. The bottom plate of the capacitor C_{911} is taken to a tap on the line output transformer that gives either a negative or positive voltage pulse. By the selection of a suitable tap, the e.h.t. can be adjusted to the value required. Because C_{913} is connected to the junction of the anode of D_{903} and cathode of D_{902}, if a negative pulse is applied to C_{911} the e.h.t. will be increased by twice the peak value of the negative pulse.

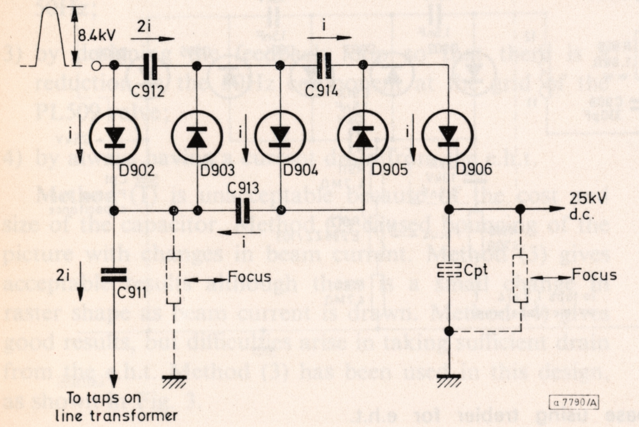

Fig.2—Practical trebler circuit

If the peak current in D_{902}, D_{904} and D_{906} during the flyback pulse is i, then the peak currents through C_{913} and C_{914} will also be i, but the peak current through C_{911} and C_{912} will be 2i. To have the same voltage drop across all the capacitors, the capacitance of C_{911} and C_{912} should be twice the value of C_{913} and C_{914}. However, to use a common type, all capacitors have been made the same value of 1·5nF. In the practical circuit, it was found that this made little difference to the performance.

The focus voltage can be taken either from the first stage of multiplication or from a resistive drain across the e.h.t., thus saving the focus rectifier. Since the impedance of the trebler is low, good focus tracking with the e.h.t. can be obtained with the former method, although the latter arrangement gives a superior performance.

A trebler unit suitable for single-standard operation is the Mullard type LP1174/1.

DESIGN OF LINE OUTPUT STAGE

To maintain acceptable convergence and colour purity in a colour receiver, the e.h.t. variation caused by changes in the picture-tube beam current must be small. One method of obtaining good e.h.t. regulation with the trebler circuit is to arrange for the line output transformer windings to be tightly coupled so that the voltage pulse fed to the trebler follows the pulse used for the v.d.r. feedback circuit.

In practice, regulation better than 2MΩ can be obtained by winding the small overwind on top of the primary. With more expensive feedback circuits using a triode, even better results can be obtained. There is, however, one serious drawback to this technique. When the diodes in the trebler circuit conduct at the peak of the flyback pulse a large current of short duration is drawn from the primary capacitance. This distorts the flyback pulse and the area of this waveform increases. To maintain equilibrium, the boosted voltage also increases, as does the scanning coil current. This, coupled with the drop in e.h.t. resulting from the flow of beam current, gives a change in scan amplitude – that is, 'breathing' with changes in beam current. It was found that for a change in picture tube beam current of from 0 to 1mA, the visible increase in scan amplitude was 7%. On a 25in picture tube this is a change in scan of 1·5in and is considered unacceptable.

A more acceptable solution is found by winding the small overwind on the opposite limb to the primary. A pulse with an approximately flat top is obtained at the end of the overwind, but there is still a sinewave across the primary. When beam current is drawn, the peak rectifying diodes conduct for a longer period because of the flat-topped shape of the waveform and, because of the leakage inductance between the primary and the overwind, the primary flyback voltage waveform is not severely distorted. This has the effect of slightly reducing the scanning coil current; the reduction compensates for the fall in e.h.t., and so the picture breathing is negligible. Typical figures of e.h.t. source impedance for a change in average beam current of 0 to 1·5mA were 1·0MΩ with a current drain across the e.h.t., and 1·5MΩ with the drain on the first stage of the multiplier. Corresponding figures for changes in picture width were 1% and 2% respectively.

To obtain the flat-topped pulse necessary for good e.h.t. regulation, the transformer is tuned to the fifth harmonic of the flyback frequency. The reflected capacitance of the overwind is so much smaller than the primary capacitance that practically all the ringing voltage is developed across the overwind, and very little across the primary. There is, therefore, no likelihood of ringing appearing on the raster even if production spreads cause detuning from the optimum conditions.

The winding specification given in the Appendix is for an unimpregnated overwind, and its self-capacitance is 54pF. If it is thought desirable to use an encapsulation the winding must be changed to allow for the increased capacitance caused by impregnation, so that it still has a self-capacitance of 54pF.

FERROXCUBE CORES

As the highest peak voltage that appears on the transformer is now reduced from 25kV to 8·4kV and there is no large overwind, the dimensions of the cores have been reduced. These reductions, with the large reduction in the overwind, give a very compact line transformer. The transformer cores are made as a U and I combination.

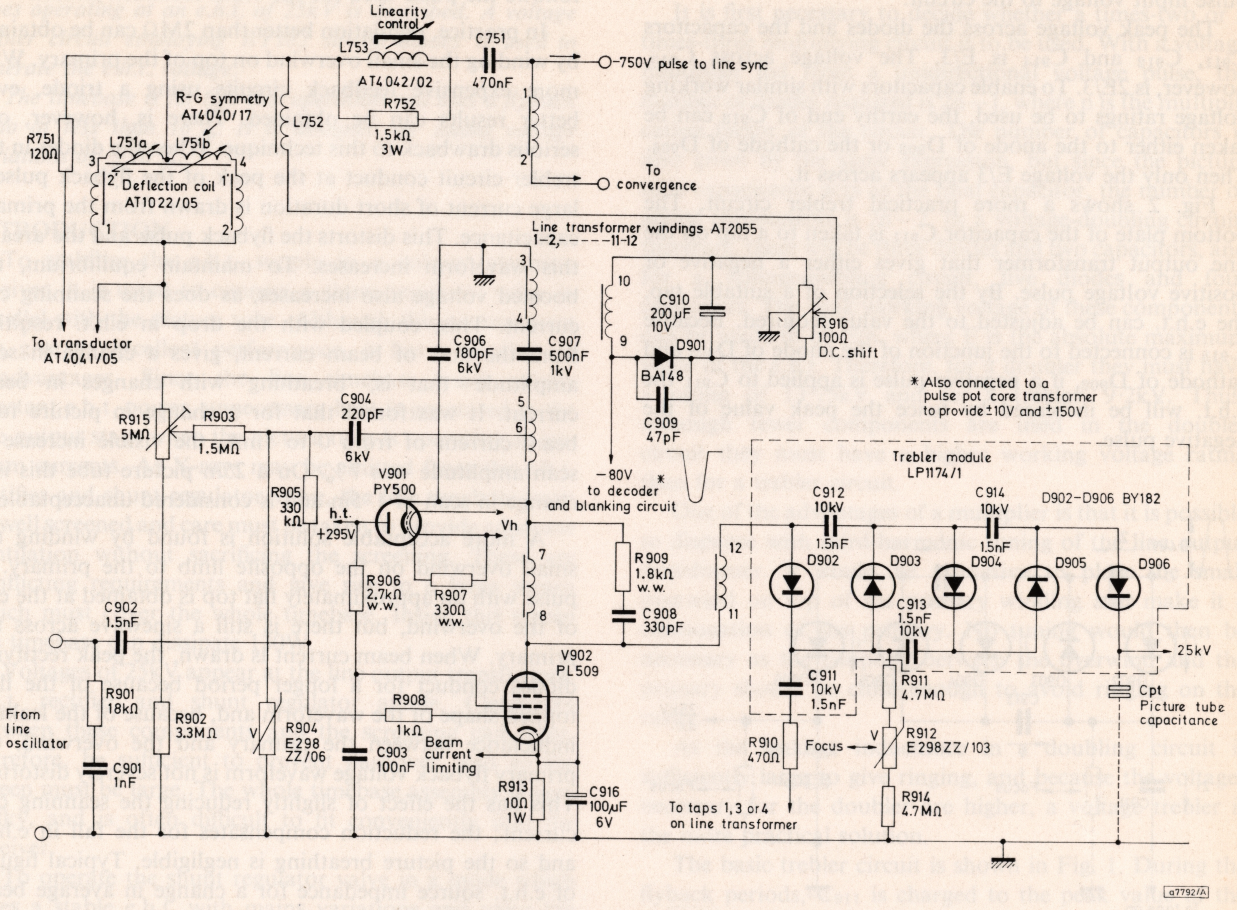
Linearity control
L753
AT4042/02
C751
470nF
-750V pulse to line sync
R-G symmetry
AT4040/17
L752
R752
1.5kΩ
3W
R751
120Ω
L751a
L751b
3
4
2'
1'
Deflection coil
AT1022/05
1
2'
1
2
To convergence
Line transformer windings AT2055
1–2,-----11-12
3
4
10
9
C910
200μF
10V
R916
100Ω
D.C. shift
D901
BA148
C909
47pF
To transductor
AT4041/05
C906
180pF
6kV
C907
500nF
1kV
* Also connected to a pulse pot core transformer to provide ±10V and ±150V
R915
5MΩ
R903
1.5MΩ
C904
220pF
6kV
5
6
−80V
to decoder
and blanking circuit
*
Trebler module
LP1174/1
C912
10kV
1.5nF
C914
10kV
1.5nF
D902–D906 BY182
V901
PY500
R905
330
kΩ
h.t.
+295V
Vh
7
12
11
8
R909
1.8kΩ
w.w.
C908
330pF
D902
D903
D904
D905
D906
C913
1.5nF
10kV
25kV
R906
2.7kΩ
w.w.
R907
330Ω
w.w.
C902
1.5nF
V902
PL509
C911
10kV
1.5nF
R911
4.7MΩ
Cpt
Picture tube capacitance
R901
18kΩ
From line oscillator
R902
3.3MΩ
V
R904
E298
ZZ/06
R908
1kΩ
C903
100nF
Beam current limiting
R910
470Ω
Focus
V
R912
E298ZZ/103
C901
1nF
R913
10Ω
1W
C916
100μF
6V
To taps 1,3 or 4 on line transformer
R914
4.7MΩ
a7792/A

Fig. 3—625 colour line timebase using trebler for e.h.t. generation

CIRCUIT DESCRIPTION

The circuit diagram of the complete line timebase is shown in Fig. 3. The circuit is for 625-line operation and uses a flyback ratio of less than 18%. The design is suitable for ±10% mains variations. The picture tube is the Mullard type A63–11X.

Voltage Trebler

Five BY182 silicon diodes (in plastic encapsulation) are used, and these have an average forward current rating of 2mA. The capacitors have a value of 1·5nF, and are Centralab components type HVA65–104.

With nominal components in the timebase, capacitor C_{911} in the trebler is connected to chassis (tap 3). The scan amplitude is adjusted by the feedback control R_{915}, and with the beam current turned to zero the e.h.t. should be 25kV. Because of component tolerances, the e.h.t. can vary from receiver to receiver.

If the e.h.t. is low, C_{911} is connected to tap 1 on the line transformer. Since a negative voltage pulse appears at this point, an e.h.t. which is nearer to the nominal value can be obtained. If the e.h.t. is high, then C_{911} is connected to tap 4 to reduce the e.h.t. Since tap 1 has a 750V negative pulse and tap 4 a 750V positive pulse, connection of C_{911} to either tap gives an adjustment in e.h.t. of ±1·5kV.

As the e.h.t. is adjustable, no width control is used, and the e.h.t. is set to match the scan.

Care must be taken in using these taps because the absolute maximum rating of the picture tube is 27·5kV. The e.h.t. can increase by 3% for a 10% increase in mains voltage, and by about a further 5% if the timebase is unsynchronised. Therefore, all receivers can be subjected to an 8% increase in e.h.t. The maximum design-centre e.h.t. will, therefore, be 27·5/1·08, or 25·5kV.

It is shown in *E.H.T. Multiplying Circuit* (page 296) that, because the absolute maximum rating of the picture tube is 27·5kV, the maximum voltage across the diodes and capacitors is 9·2kV. Under fault conditions or during the initial setting-up in production, if the e.h.t. rises above 27·5kV, no diode failures should occur. However, if the feedback control R_{915} is misadjusted or a fault occurs in this circuit, then grid current may flow in the PL509 and the valve will operate below the knee of the I_a/V_a characteristic. Measurements have shown that under these conditions in a typical receiver the e.h.t. rises to 30kV. The p.i.v. rating of the BY182 diode is sufficient to allow for faults or circuit misadjustments.

The BY182 will also withstand the surge which occurs if the picture tube flashes over or the e.h.t. is momentarily shorted to chassis. The 470Ω resistor R_{910} in series with C_{911} (Fig. 3) limits the current through this capacitor in the event of flashover. Morganite type W is suitable for R_{910}.

Pincushion Raster Correction

To correct for the E–W pincushion raster distortion the line scanning coil current must be modulated at field frequency. This is achieved by the Mullard transductor AT4041/05. Because of the impedance of the boost capacitor at 50Hz and the forward resistance of the PY500, the voltage and current waveforms of the line transformer will also be modulated. At low beam currents this gives rise to a 50Hz modulation of the e.h.t.

There are several methods of overcoming this effect:

1) by using a large value of boost capacitor—about 10μF;

2) by giving the feedback loop a long time–constant at 50Hz;

3) by designing the feedback loop so that there is a reduction in the 50Hz component at the grid of the PL509 valve;

4) by always having a current drain from the e.h.t.

Method (1) is unacceptable because of the cost and size of the capacitor. Method (2) caused bouncing of the picture with changes in beam current. Method (3) gives acceptable results although there is a small change in raster shape as beam current is drawn. Method (4) gives good results, but difficulties arise in taking sufficient drain from the e.h.t. Method (3) has been used in this design, as shown in Fig. 3.

Focus Potential

Two methods of obtaining the focus potential are shown in Fig. 2, either from a resistive drain across the e.h.t., or from the first stage of the multiplier. The first method gives better tracking of the focus and e.h.t. potential, but is the more expensive arrangement. However, obtaining the focus potential from the first stage of the multiplier gives acceptable performance even if the focus is adjusted at a low beam current. At 1·5mA average beam current, the focus potential is within 50V of the value for optimum focus.

In Fig. 3 the focus potential is obtained from a tap on a v.d.r. (E298ZZ/103). Resistors R_{911} and R_{914} are placed

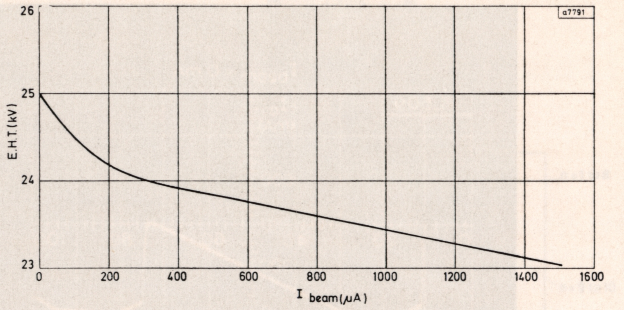

Fig. 4—E.H.T. regulation

in series with the v.d.r. to protect it against overvoltage conditions, when the current and dissipation could be excessive. The e.h.t. regulation curve with this arrangement is shown in Fig. 4.

Picture Shift

As no shunt regulator valve is used, the average current taken by the line output pentode will vary as the beam current changes. This means the d.c. shift network cannot be placed in the cathode of the PL509.

Shift is obtained by rectifying the scan voltage across winding 9–10. This voltage is smoothed and applied to a centre-tapped potentiometer (R_{916}) which gives continuous two-way shift without switching.

Convergence

The convergence circuit (Ref. 2) requires a negative-going sawtooth current. For this purpose, the primary of the line transformer has been split at tap 2/3. One side is connected to the convergence circuit, and the other to chassis.

Oscillator

A flywheel oscillator (Ref. 3), uses a PCF802. The output voltage is shaped by an RC network and the values of R_{901} and C_{901} (Fig. 3) are chosen so that the booster diode is just conducting at the end of scan with zero picture-tube current.

ADVANTAGES OF VOLTAGE-TREBLER CIRCUIT

The advantages of the voltage-trebler circuit compared with a shunt-regulator circuit (Ref. 1) are:

1) no shunt regulator valve and associated components;

2) no e.h.t. valve rectifier;

3) e.h.t. overwind greatly reduced in size;

4) smaller ferrite core, more compact transformer;

5) no X-radiation, therefore simpler screening;

6) no third-harmonic tuning, therefore no coupling winding or tuning inductors;

7) safer line output transformer, as maximum peak voltage is 8·4kV compared with 25kV;

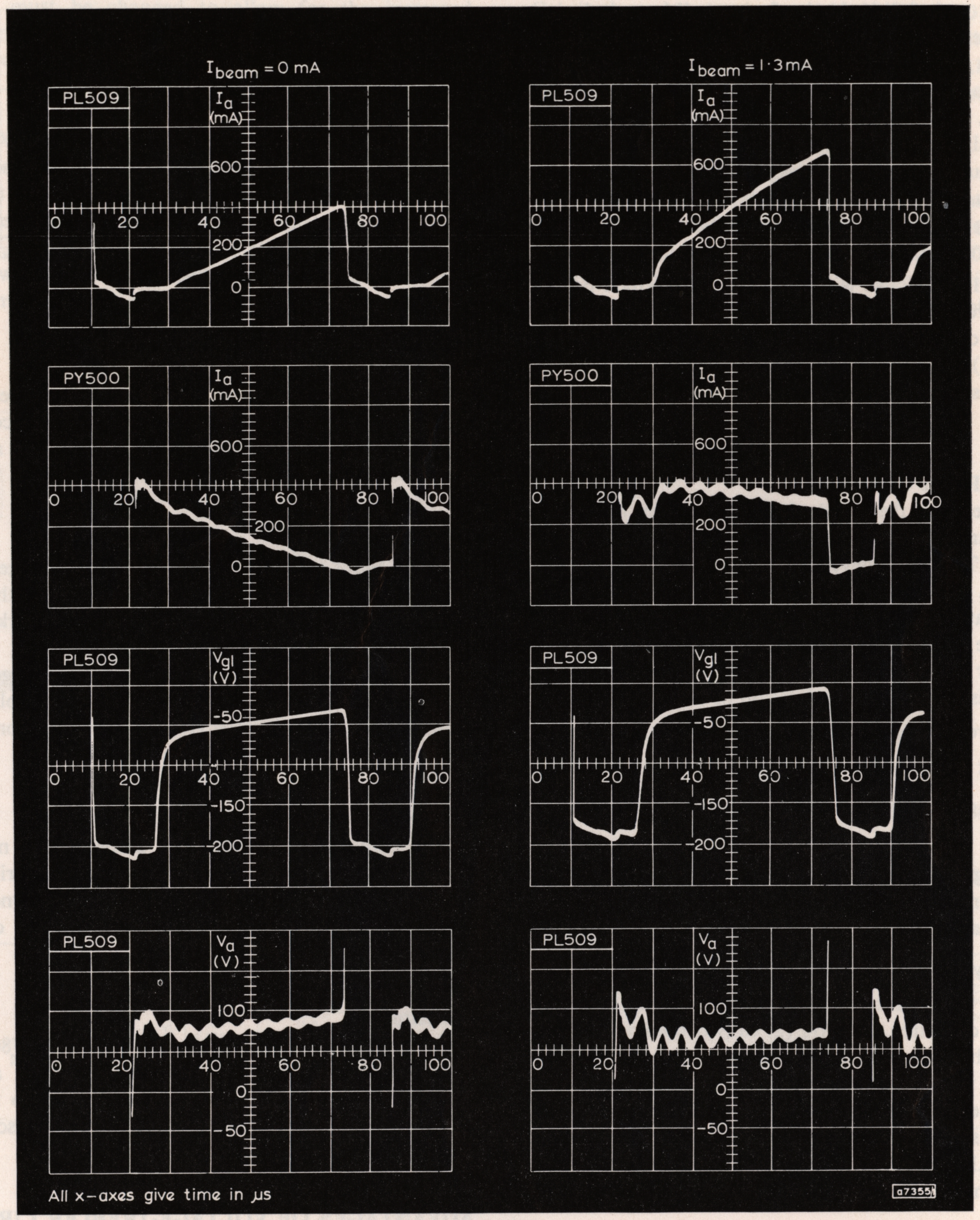

Fig. 5—PL509 and PY500 waveforms for 625-line operation

8) less heat in line transformer screening can;

9) less onerous operating conditions for line output valve;

10) no line transformer loading coil or desaturating coil;

11) no width control coil;

12) no focus valve rectifier and associated components.

Against these advantages one factor must be considered. Since the e.h.t. regulation is worse than with a shunt regulator, the light output for a given beam current in the picture tube will be slightly less.

It is important, with the trebler circuit, to operate from a power supply with a low source impedance, otherwise the e.h.t. regulation will worsen. A further effect is a variation in h.t. line voltage with changes in beam current which may have detrimental effects on other circuits. The power supply used for this design had a source impedance of 90Ω and had little effect on the e.h.t. regulation.

VALVE OPERATING CONDITIONS

The measurements in Table 1 were carried out with nominal PL509 and PY500 valves in the circuit shown in Fig. 3. Current and voltage waveforms for these valves are shown in Fig. 5.

TABLE 1
Valve Operating Conditions

I_{beam}	0	1·0	1·5	mA
*V_{supply}	295	285	280	V
E.H.T.	25·0	23·4	23·0	kV
†Overscan	9			%
Flyback ratio	17·2	17·8	18·0	%
$V_{boosted}$: (with respect to chassis)	820	805	797	V
PL509				
$I_{a(av)}$	152	256	305	mA
$I_{g2(av)}$	15	25	29	mA
$v_{a(pk)}$	6·9	6·7		kV
$i_{a(pk)}$	410	615		mA
p_a	12·0	16·1		W
p_{g2}	3·8	5·5		W
$V_{a(end\ of\ scan)}$	92	74		V
PY500				
$I_{a(av)}$	152	256	305	mA
$i_{a(pk)}$	440	400		mA
$i_{a(end\ of\ scan)}$	20	180		mA
$v_{a-(pk)}$	5·3	5·2		kV

*Source impedance 90Ω

† Overscan over the faceplate phosphor, measured at beam current of 50µA. For a beam current change from 0 to 1·5mA, the picture width increases by approximately 2%.

REFERENCES

1. BOULTON, P. G., KING, D. J., LAMMERS, J., SKELTON, D., 'Convergence, Raster-correction, and Timebase Circuits for 25in Colour Tube', **Mullard Technical Communications**, Vol. 9, No. 83, September 1966, Part 3, pp. 69. to 72.
2. KING, D. J., THOMSON, E. C., 'Pincushion Correction and Convergence Circuits', **Mullard Technical Communications**, Vol. 10, No. 97, January 1969, pp. 217 to 222.
3. GANDER, M. C., HAMPSON, L., 'Luminance, colour-difference output, synchronising and a.g.c. circuits', to be published shortly in **Mullard Technical Communications**.

APPENDIX

Wound Components

Scanning Coils
Mullard AT1022/05, which has the following line coil specification:

Inductance at 1kHz	2·9mH
Resistance at 25°C	2·9Ω
Peak-to-peak current for edge-to-edge scan at 25kV	2·6A

Linearity Control
Mullard AT4042/02

R-G Symmetry Control
Mullard AT4040/17

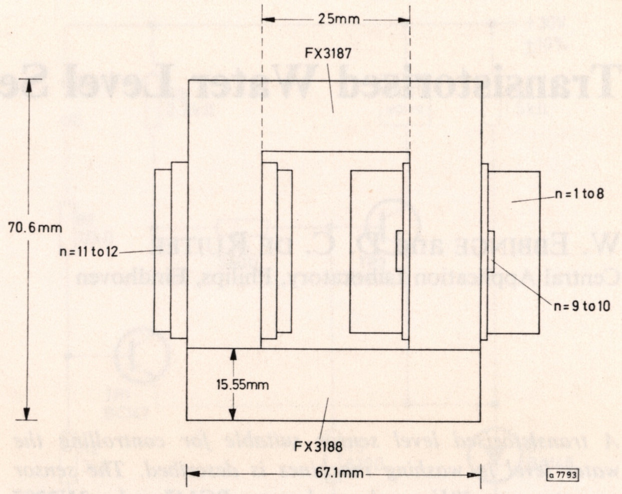

Fig. 6—Cross section of transformer showing position of coils on Ferroxcube core

Coil L_{752}
Winding: 800 turns of 30 s.w.g. enamelled copper wire with F (fine) covering; wound 100 turns/layer
Core: FX1054

Line Output Transformer (Figs. 3 and 6)
Former for windings 1-10: SRBP, internal diameter, 19·1mm; wall. 0·8mm; length, 35mm
Former for windings 11-12 SRBP, internal diameter, 19·1mm; wall, 3·2mm; length, 35mm
Winding 1-8 775 turns tapped at 80, 160, 238 and 595 turns; at 80 and 160 turns leads are separated; wound 54 turns/layer with 28 s.w.g. enamelled copper wire with F covering
Winding 9-10 9 turns of 28 s.w.g. enamelled copper wire with F covering
Winding 11-12 210 turns of 34 s.w.g. enamelled copper wire with F covering; wound 70 turns/layer
Interleaving: For all windings, 2 x 0·002in cellulose acetate butrate foil between each layer.
Cores: U core FX3187; I bar FX3188
Airgap: 2 x 0·008in paper

The AT2055 transformer is based on this winding specification, and is illustrated in Fig. 6.

Transistorised Water Level Sensor

W. EBBINGE and D. C. DE RUITER
Central Application Laboratory, Philips, Eindhoven

A transistorised level sensor suitable for controlling the water level in washing machines is described. The sensor operates on a 30V supply, and uses a BC147 and a 2N2297 transistor. The latter directly operates a 28V 280mA electromagnetic inlet valve, and the sensing elements are simple electrodes that can be sealed into the wall of an open vertical tube. This sensor is free from the inherent inaccuracy of conventional sensors that operate by pressure build-up in an air column and that are affected by water temperature.

INTRODUCTION

A widely-used water level sensor in washing machines is a device operated by the pressure build-up in an air column caused by the rising water in a vertical tube that communicates with the washing barrel. The air pressure is relayed by a rubber membrane to one or more microswitches whose initial tensions determine the pressures at which they are switched. A limitation with this type of level control is that at a specific pressure the air column over the water level in the tube depends also on the water temperature. As a result, hot water is maintained at a lower level than cold water.

The transistorised level sensor operates on a change in resistance between two electrodes when the water level reaches both of them. They are sealed into the wall of an open vertical tube communicating with the washing barrel. One electrode for any level to be controlled is situated at that level and in every instance it co-operates with a common electrode of opposite polarity. A voltage variation, caused by the varying resistance between the common electrode and the electrode at the level to be controlled, is amplified to control an electromagnetic inlet valve. The transistorised amplifier can easily be integrated with a complex system of other electronic controls.

DESIGN CONSIDERATIONS

The supply voltage for the amplifier is 30V d.c., which is also used for the other sensors in washing machines. Supply voltage variations do not affect the correct working of the amplifier.

The water flow is admitted when the coil of the inlet valve is energised (28V, 280mA). Fig. 1 shows the dependence of the resistance between two electrodes, immersed at a distance of 120mm in distilled, mains and dirtied water, on the voltage between them. The measurements were made with stainless steel and with aluminium electrodes having total areas of 1000mm^2 and 50mm^2. From Fig. 1 it can be seen that even for pure water, an electrode area of 50mm^2 is sufficient to make the resistance between the electrodes fall below 20kΩ on the condition that for d.c. the voltage between the electrodes is greater than 5V. This value also applies to the electrode conditions in a washing machine. When water is in contact with only one of the electrodes, the resistance is greater than 200kΩ.

The BC147 transistor is eminently suitable as a preamplifier because of its very low I_{CBO} (collector-base cut-off current, emitter open-circuit). It drives a 2N2297 transistor whose maximum collector current of 1A is ample to energise the coil of the inlet valve; therefore, a relay is not required. A BA148 diode provides a bias voltage (about 0·6V) for the emitters, to allow reduction of their collector current values to zero. It is possible that a different bias voltage will be necessary when the level sensor is integrated with a completely electronic control system because the level sensor must be able to override other sensors.

CIRCUIT DESCRIPTION

Fig. 2 is the circuit diagram of a complete level sensor intended for use in a washing machine. Points D and E represent the common and the level-sensing electrode. A high resistance between these electrodes means a low current through R_2, so that the voltage at the base of TR_1 is low; consequently, TR_1 is non-conducting. The values of resistors R_3, R_4 and R_5 are calculated in such a way as to make TR_2 then conducting. Hence the coil of the inlet valve is energised, and the water level rises until it has reached both electrodes D and E. The resistance between these electrodes then suddenly drops, causing the current through R_2 to increase. As a result, the voltage at the base of TR_1 rises so that this transistor becomes fully conductive; the collector voltage will then be a certain small amount $V_{CE(TR1)}$ above its emitter voltage. The voltage divider R_4, R_5, and voltages $V_{CE(TR1)}$ and V_D (diode voltage) must be related in such a way that the V_{BE} (cut-off voltage) of TR_2 is then obtained. Consequently, the coil of the inlet valve is de-energised, and the water supply is cut off.

COMPONENT VALUES

The inlet valve is completely cut off when the current through its coil (the collector current of TR_2) has dropped to 2mA. The 2N2297 characteristics are such that for a collector current of 2mA and a V_{CE} of 10V, the h_{FE} (large signal common emitter current gain) is 40 so that the base current is $2\times10^{-3}/40=50\mu A$. However, the V_{CE} is 30V, making the base current somewhat lower, about 40µA. The V_{BE} is then about 200mV.

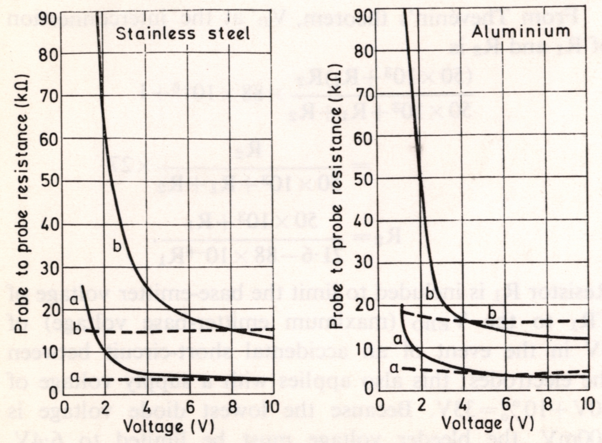

Distilled water with a conductivity of 400µmho/mm

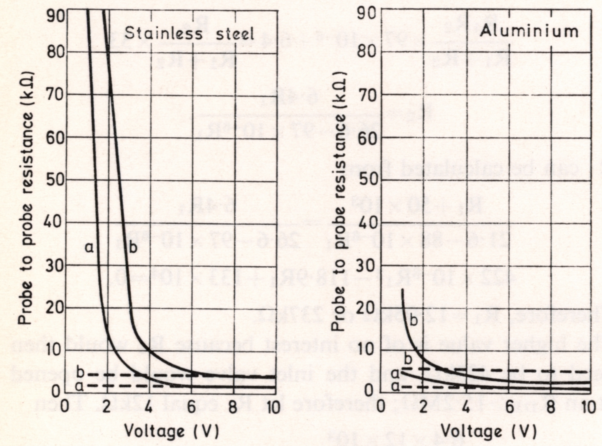

Mains water

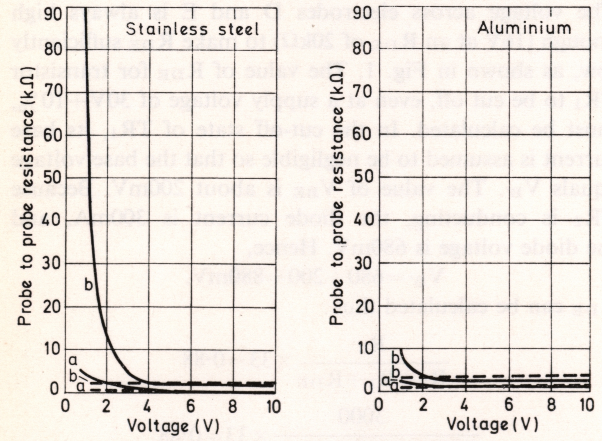

Dirtied washing water with a conductivity of 4000µmho/mm

a7839

Fig. 1—Water resistance between electrodes, plotted against applied voltage.
Curves a, 1000mm^2 total surface area of electrodes
Curves b, 50mm^2 total surface area of electrodes
Distance between electrodes 120mm
Broken curves for 50Hz a.c. (r.m.s. value)
Solid curves for d.c.

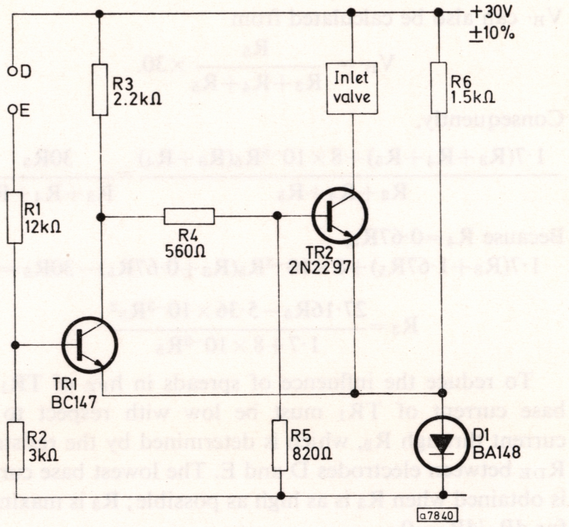

Fig. 2—Water level sensor

The full energising current of the coil is 280mA. For this collector current, the V_{CE} is 600mV, the base current 8mA, and the V_{BE} about 1V. For adequate stabilisation of the emitter voltages the current through diode D_1 must not be less than about 20mA, which is ensured by a resistance of 1·5kΩ, R_6. The forward voltage V_F is then 400mV; for 300mA the V_F is 680mV.

Calculation of R_3, R_4 and R_5

When the collector current of TR_2 is 2mA, TR_1 conducts making its V_{CE} 600mV. Its collector voltage is then

$$V_C=V_{CE(TR1)}+V_D=0{\cdot}6+0{\cdot}4=1V.$$

The base voltage of TR_2, for a collector current of 2mA, is

$$V_{BE}+V_D=0{\cdot}2+0{\cdot}4=0{\cdot}6V.$$

Consequently, $R_5:(R_4+R_5)=0{\cdot}6:1$, hence $R_5=1{\cdot}5R_4$ and $R_4=0{\cdot}67R_5$.

When the collector current of TR_2 is 280mA, the base current is 8mA. TR_1 is then cut off, and the base of TR_2 is connected to a bleeder R_3, R_4 and R_5. The base voltage of TR_2 at a collector current of 280mA is

$$V_{D(300mA)}+V_{BE}=0{\cdot}68+1\simeq1{\cdot}7V.$$

The open bleeder voltage $V_{B'}$ at the interconnection of R_4 and R_5 can be calculated from Thevénin's theorem. The base current of TR_2 flows through R_5 in parallel with R_3+R_4, the resistance being

$$\frac{R_5(R_3+R_4)}{R_3+R_4+R_5}.$$

The voltage drop across R_5 in parallel with R_3+R_4 is

$$\frac{8\times10^{-3}\times R_5(R_3+R_4)}{R_3+R_4+R_5}.$$

Therefore,

$$V_{B'}=1{\cdot}7+\frac{8\times10^{-3}R_5(R_3+R_4)}{R_3+R_4+R_5}.$$

$V_{B'}$ can also be calculated from

$$V_{B'}=\frac{R_5}{R_3+R_4+R_5}\times 30.$$

Consequently,

$$\frac{1{\cdot}7(R_3+R_4+R_5)+8\times10^{-3}R_5(R_3+R_4)}{R_3+R_4+R_5}=\frac{30R_5}{R_3+R_4+R_5}.$$

Because $R_4=0{\cdot}67R_5$,

$$1{\cdot}7(R_3+1{\cdot}67R_5)+8\times10^{-3}R_5(R_3+0{\cdot}67R_5)-30R_5=0$$

$$R_3=\frac{27{\cdot}16R_5-5{\cdot}36\times10^{-3}R_5^2}{1{\cdot}7+8\times10^{-3}R_5}.$$

To reduce the influence of spreads in h_{FE} of TR_1 the base current of TR_1 must be low with respect to the current through R_2, which is determined by the resistance R_{DE} between electrodes D and E. The lowest base current is obtained when R_3 is as high as possible; R_3 is maximum for $dR_3/dR_5=0$.

$$\frac{dR_3}{dR_5}=\frac{(1{\cdot}7+8\times10^{-3}R_5)(27{\cdot}16-10{\cdot}72\times10^{-3}R_5)}{(1{\cdot}7+8\times10^{-3}R_5)^2}-\frac{(27{\cdot}16R_5-5{\cdot}36\times10^{-3}R_5^2)8\times10^{-3}}{(1{\cdot}7+8\times10^{-3}R_5)^2}$$

Hence, $42{\cdot}9R_5^2+18{\cdot}2\times10^3R_5-46{\cdot}1\times10^6=0$, so that

$R_5=850\Omega$ (nearest preferred value 820Ω)

$R_4=0{\cdot}67\times820=550\Omega$ (nearest preferred value 560Ω)

$$R_3=\frac{27{\cdot}16\times820-5{\cdot}36\times10^{-3}\times820^2}{1{\cdot}7+8\times10^{-3}\times820}=2260\Omega$$

(nearest preferred value $2{\cdot}2k\Omega$).

Calculation of R_1 and R_2

When TR_2 is cut off, TR_1 must be fully conductive, making its collector-emitter voltage 600mV. Because the diode voltage is then 400mV, the collector voltage is 1V. The collector current of TR_1 is $(30-1)/2200=13{\cdot}2$mA. At this collector current, the maximum base current (for $h_{FE}\simeq150$) is about 88μA. The base-emitter voltage is about 600mV and the bleeder voltage 1V.

Transistor TR_1 must conduct when the resistance between electrodes D and E is less than $20k\Omega$, even at a supply voltage of $30V-10\%=27V$. However, when an R_{DE} of $20k\Omega$ is used in the subsequent calculations, the calculated values of R_1 ($3{\cdot}9k\Omega$) and R_2 (953Ω) make the sensor switch on at $20k\Omega$, as calculated, and switch off at $30{\cdot}8k\Omega$. The value of $30{\cdot}8k\Omega$ is far below the tolerated switch-off value of $200k\Omega$, the latter already being lower than the measured value. Because the resistance of very pure water may be $50k\Omega$, it is worth calculating R_1 and R_2 for this value to determine how much less than $200k\Omega$ the switch-off value of R_{DE} can become.

From Thevénin's theorem, V_B' at the interconnection of R_1 and R_2 is

$$\frac{(50\times10^3+R_1)R_2}{50\times10^3+R_1+R_2}\times88\times10^{-6}+1$$

$$=\frac{R_2}{50\times10^3+R_1+R_2}\times27$$

$$R_2=\frac{50\times10^3+R_1}{21{\cdot}6-88\times10^{-6}R_1}.$$

Resistor R_1 is included to limit the base-emitter voltage of TR_1 to the V_{EBO} (maximum emitter-base voltage) of 6V in the event of an accidental short-circuit between the electrodes; this also applies with a supply voltage of $30V+10\%=33V$. Because the lowest diode voltage is 400mV, the bleeder voltage must be limited to 6·4V. The collector current for a 33V supply is $(33-1)/2200=14{\cdot}5$mA, and the base current is 97μA. $V_{B'}$ is then

$$\frac{R_1R_2}{R_1+R_2}\times97\times10^{-6}+6{\cdot}4=\frac{R_2}{R_1+R_2}\times33$$

$$R_2=\frac{6{\cdot}4R_1}{26{\cdot}6-97\times10^{-6}R_1}.$$

R_1 can be calculated from

$$\frac{R_1+50\times10^3}{21{\cdot}6-88\times10^{-6}R_1}=\frac{6{\cdot}4R_1}{26{\cdot}6-97\times10^{-6}R_1}$$

$$422\times10^{-6}R_1^2-118{\cdot}9R_1+133\times10^4=0.$$

Therefore, $R_1=12{\cdot}05k\Omega$ or $237k\Omega$.

The higher value is of no interest because R_2 would then need to be $423k\Omega$, and the inlet valve would be opened at an $R_{DE}>15{\cdot}2M\Omega$; therefore let R_1 equal $12k\Omega$. Then

$$R_2=\frac{6{\cdot}4\times12\times10^3}{26{\cdot}6-90\times10^{-6}\times13\times10^3}=3{\cdot}015k\Omega,\ \text{say } 3k\Omega.$$

The voltage across electrodes D and E is always high enough (16V at an R_{DE} of $20k\Omega$) to make R_{DE} sufficiently low, as shown in Fig. 1. The value of R_{DE} for transistor TR_1 to be cut off, even at a supply voltage of $30V+10\%$, must be calculated. In the cut-off state of TR_1, its base current is assumed to be negligible so that the base voltage equals $V_{B'}$. The value of V_{BE} is about 200mV. Because TR_2 is conducting, the diode current is 300mA, and the diode voltage is 680mV. Hence,

$$V_{B'}=680+200=880\text{mV}.$$

R_{DE} can be calculated thus:

$$\frac{R_2}{R_2+R_1+R_{DE}}\times33=0{\cdot}88$$

$$\frac{3000}{3000+12000+R_{DE}}\times33=0{\cdot}88$$

$$R_{DE}=97{\cdot}5k\Omega.$$

Consequently, an R_{DE} value greater than $200k\Omega$ definitely will make TR_1 non-conductive.